



Cellular automaton simulations for mixed traffic with erratic motorcycles' behaviours

Lawrence W. Lan^{a,1}, Yu-Chiun Chiou^{b,*}, Zih-Shin Lin^{b,2}, Chih-Cheng Hsu^{b,2}

^a Department of Global Marketing and Logistics, MingDao University, 369 Wen-Hua Road, Peetow, Chunghua 52345, Taiwan

^b Institute of Traffic and Transportation, National Chiao Tung University, 4F, 118 Sec.1, Chung-Hsiao W. Road, Taipei 10012, Taiwan

ARTICLE INFO

Article history:

Received 29 October 2009

Received in revised form 31 December 2009

Available online 28 January 2010

Keywords:

Cellular automaton

Mixed traffic

Motorcycle

ABSTRACT

Modeling mixed traffic composed of motorcycles can be a challenging issue because many erratic motorcyclists may not follow the lane disciplines, particularly when traffic is congested. Based upon the refined cellular automaton (CA) model recently developed by the authors [L.W. Lan, Y.C. Chiou, Z.S. Lin, C.C. Hsu, *Physica A* 388 (2009) 3917–3930], this paper further proposed a sophisticated CA model to elucidate the erratic motorcycle behaviours in mixed traffic contexts. In addition to the conventional moving forward and lane-change rules, the sophisticated CA model also explicated the lateral drift behaviour for cars moving in the same lane, the lateral drift behaviour for motorcycles breaking into two moving cars, and the transverse crossing behaviour for motorcycles through the gap between two stationary cars in the same lane. Fundamental diagrams and space-time trajectories for vehicles with various car-motorcycle mixed ratios are demonstrated.

© 2010 Elsevier B.V. All rights reserved.

1. Introduction

Recently, cellular automaton (CA) modelling has been popularly used to elucidate traffic flows. Nagel and Schreckenberg [1] first proposed the prominent NaSch model in early 1990s in which they devised a simple yet efficient algorithm to describe the complex traffic phenomena. Vehicular positions, speeds, accelerations as well as times are all treated as discrete variables. A single lane is represented by one-dimensional lattice whereas each of the lattice sites represents a cell, which can be either empty or occupied by at most one vehicle at a given instant of time step. As time advances, each vehicle evaluates the impact of nearby neighbours and takes adequate action via several simple rules in each time step. To capture more important traffic features or to be more in line with the realistic traffic behaviour, numerous modified CA models were developed or extended on the basis of the NaSch model in the past decade (e.g., Refs. [2–9]). An excellent and compressive introduction of the advance in traffic modelling in late-twentieth century, especially for two-lane traffic behaviours and CA modelling can be found in Ref. [10]. Recently, Kerner and his associates further proposed the famous three-phase traffic theory [11–14]. However, these modified models mainly dealt with pure traffic (only one type of vehicle such as cars) on freeways. Incorporation of more realistic CA rules into the simulation of mixed traffic (various types of vehicles such as cars, motorcycles, buses) on urban streets or surface roads is comparatively less addressed, perhaps due to the restraint circumvented by the coarse cell systems defined. Although the mixed traffic contexts hitherto are seldom

* Corresponding author. Tel.: +886 2 23494940; fax: +886 2 23494953.

E-mail addresses: lawrencelan@mdu.edu.tw (L.W. Lan), ycchiou@mail.nctu.edu.tw (Y.-C. Chiou), simon.tt93g@nctu.edu.tw (Z.-S. Lin), charles.tt92g@nctu.edu.tw (C.-C. Hsu).

¹ Tel.: +886 4 8876660x7500; fax: +886 4 8879013.

² Tel.: +886 2 23494995; fax: +886 2 23494953.

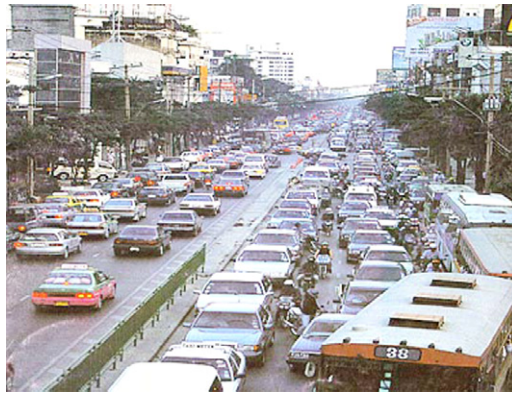


Fig. 1. Erratic motorcyclists in urban mixed traffic.

studied through CA modelling, an in-depth understanding of mixed traffic behaviour can be imperatively important in many Asian cities where motorcycles are prevailing.

Most existing CA models utilized the comparatively coarse cell system defined by the NaSch model [1]. Therefore, each lane only allowed to be occupied by a single vehicle laterally. One crucial defect aroused from such a coarse cell system is that it would be difficult to implement the mixed traffic simulations where vehicles have different sizes (length and width) and/or possess distinct behaviour. For example, it is ubiquitous in many Asian urban streets that motorcycles oftentimes move concurrently with the cars by sharing the “same lane” (see Fig. 1). Some erratic motorcyclists do not even follow the lane disciplines at all. They may make lateral drifts breaking into two moving cars. Once blocked by the front vehicles, they even make wide transverse crossings through the gap between two stationary cars in the same lane, in order to keep moving forward. In this circumstance, obviously, the conventional coarse cell system is deficient to describe various vehicle sizes with their coupled interactions.

Another shortcoming of the coarse cell system is the derived low resolution which stands as the crucial barrier for implementing the CA into urban traffic simulation. In urban streets, the speed limits are usually low. For instance, if the speed limit is 60 kph, there would only be three speed options available for any vehicle—0, 28 kph and 56 kph provided that the cell system in the NaSch model (7.5 m) is used for CA simulation. This is apparently not so practical if one wishes to scrutinize in detail the microscopic traffic features or to trace the realistic behaviour of an individual vehicle. Furthermore, most existing CA works only considered basic heterogeneity among vehicles, including various speed limits and/or different vehicle lengths. For instance, Nagel [3], Chowdhury et al. [4], Ebersbach et al. [15] and Wang et al. [16] analyzed the impact of partial vehicles equipped with lower or higher maximum speed in the traffic flow. Ez-Zahraouy et al. [17] evaluated the effect of mixture lengths of vehicles on the traffic flow in a single-lane context. In Knospe's et al. [6] paper, a two-lane system with smaller cell sizes and different types of vehicles were studied. Kerner [18] further evaluated both the effects of different vehicle lengths and various maximum speeds. In these CA models, except that by Knospe et al. [6], Wang et al. [16] and Kerner [18], the small vehicles occupy one cell, while the big ones take two cells, but none ever take the impact of vehicular widths into consideration. The only existing effort taking vehicular width into account is perhaps by Meng et al. [19], who tried to divide a single-lane into three sub-lanes and thus allowed the introduction of motorcycles into simulation.

Existing studies of urban traffic CA simulations can be categorized into two approaches. The first approach considers an abstract network which assumes a two-dimensional lattice and focuses on the investigation of phase transitions [20–26]. The second approach tries to describe the real-world traffic prevailing on the surface roadways in populated cities [27–31]. Since these models basically followed the NaSch's coarse cell system, inevitably the vehicular speeds had merely three options (0, 1, 2) to cope with the prevailing urban speed limits [28,31]. Moreover, none of these CA models ever attempt to rectify the abrupt deceleration of vehicles when approaching the intersection or the upstream front of traffic jams.

Upon above, Lan and Chang [32] first developed an inhomogeneous CA model to elucidate the interacting movements of cars and motorcycles in urban street mixed traffic contexts. Hsu et al. [33] further extended this concept and introduced the generalized spatiotemporal definitions for occupancy, flow, and speed to precisely capture the collective behaviour of traffic features. They also introduced a refined common unit (CU) system to represent a “fine cell” and a “fine site”, which can respectively gauge the non-identical vehicular widths and lengths as well as the non-identical lane widths. Their simulation results demonstrated that the proposed refined CA model is capable of capturing some essential features of traffic flows. One important advantage of the refined CU system is that the “resolution” of the simulation results has been largely enhanced. Hence, the variation of vehicular speeds as well as the coupled positions update can be revealed more precisely. Also the effects of both vehicle width and lane width, besides the effects of vehicle length, can be accounted for. More recently, Lan et al. [34] revised the conventional CA particle-hopping velocity variation to be a piecewise-linear velocity variation so as to more realistically reflect the genuine vehicle movement. They also introduced, as inspired by Lee et al. [35] and Knospe et al. [6], the concept of limited deceleration capability of vehicles into their CA simulations. According to their

results, the unrealistic deceleration behaviour was successfully rectified; besides, the three-phase traffic patterns proposed by Kerner [11–14] and the associated phase transitions were also effectively displayed in their simulations.

Based on the refined CA models proposed by Lan et al. [34], this paper further developed the sophisticated CA model to elucidate the mixed traffic flow comprising cars and motorcycles. Taking the advantages of enhanced resolution of the refined cell system, more realistic traffic speeds prevailing in urban streets with various vehicular sizes (width and length) can be simulated. Therefore, in addition to the conventional moving forward and lane-change rules, the sophisticated CA model also explicated the lateral drift behaviour for cars moving in the same lane, the lateral drift behaviour for motorcycles breaking into two moving cars, and the transverse crossing behaviour for motorcycles through the gap between two stationary cars in the same lane. The simulations on such mixed traffic behaviour are thoroughly examined under various scenarios.

The rest of this paper is organized as follows. The concept of generalized traffic parameters and the proposed new CA rules are briefly narrated in Section 2, wherein lateral drift update rules for cars and motorcycles, the transverse drift update rules for motorcycles will be carefully elucidated. The simulations for mixed traffic contexts are reported in Section 3. Conclusions and suggestions for future studies then follow.

2. Models

2.1. Common unit for cells and sites

The concept of “common unit” (CU) was first introduced by Hsu et al. [33] to describe different vehicle types and their required clearances for safe movement in the context of various widths of lanes or roadways. In this study a fine grid of 1×1.25 m is defined as the CU for cells (vehicles) and sites (roadway spaces). For instance, for a two-lane road with 3.75 m width in each lane, the road width can be represented by 6 CUs. Therefore, for safe movement with acceptable clearances, a car is represented by 6×2 CUs, always occupying 12 CUs of the roadway space, whereas a motorcycle is represented by 2×1 CUs, always taking up 2 CUs of the roadway space.

2.2. Spatiotemporal traffic variables

According to Lan et al. [34], the generalized traffic parameters, including occupancy, $\rho(S)$, traffic flow $q(S)$ as well as the space-mean speed $v(S)$ over a simulated 3D space S are defined respectively as follows:

$$\rho(S) = \frac{\sum N_0(t) \Delta t}{\sum N \Delta t} = \frac{t(S)}{|S|} \quad (1)$$

$$q(S) = \frac{\sum M_0(x) \Delta x}{\sum T \Delta x} = \frac{d(S)}{|S|} \quad (2)$$

$$v(S) = \frac{q(S)}{\rho(S)} = \frac{d(S)}{t(S)}. \quad (3)$$

The above-generalized traffic parameters are used in this study to depict the global behaviour of traffic flow patterns in the following CA simulations. In addition, to facilitate the readability of the model, a notation table summarizing all the variables and parameters in this study is given in Appendix (Table A.1).

2.3. Forward rules for cars and motorcycles

The forward rules utilized in this study follow those proposed by Lan et al. [34] who took limited deceleration capability into consideration. The proposed forward update rules apply to both cars and motorcycle and can be described as the following seven steps.

Step 1: Determination of the randomization probability:

$$p(v_n(t), t_h, t_s, S_{n+1}(t)) = \begin{cases} p_b : \text{if } S_{n+1} = 1 \text{ and } t_h < t_s \\ p_0 : \text{if } v_n = 0 \text{ and } t_{st} \geq t_{k,c} \\ p_d : \text{in all other cases.} \end{cases} \quad (4)$$

In this study, $k = 1$ represents cars, $k = 0$ for motorcycles.

Step 2: Acceleration. Determine the speed of vehicles in next time step:

$$\begin{aligned} \text{if } (S_{n+1}(t) = 0) \text{ or } (t_h \geq t_s) \text{ then } v_n(t+1) &= \min(v_n(t) + a_k, v_{k,\max}) \\ \text{else } v_n(t+1) &= v_n(t). \end{aligned} \quad (5)$$

Step 3: Deceleration. If $v_{n+1}(t+1) < v_n(t+1)$, check the following safety criteria to determine speed at the next time step:

$$x_n(t+1) + \Delta + \sum_{i=1}^{\tau_n(c_n(t+1))} (c_n(t+1) - Di) \leq x_{n+1}(t+1) + \sum_{i=1}^{\tau_n(c_n(t+1))} v_{n+1}(t+1). \quad (6)$$

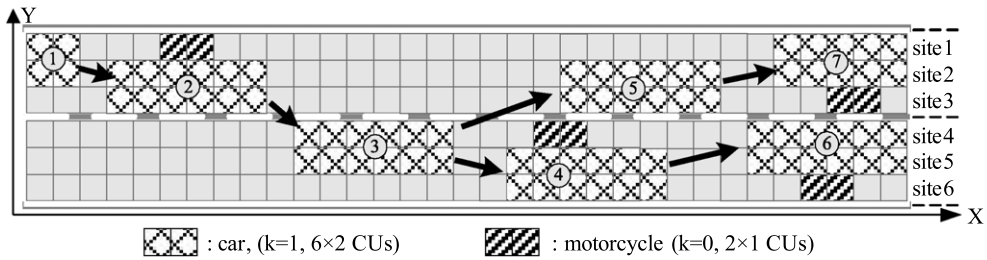


Fig. 2. Lateral movements for cars in mixed traffic: lane-change and lateral drift.

Step 4: Randomization:

$$\text{if } (\text{rand}() < p) \text{ then } v_n(t + 1) = \max(v_n(t + 1) - 1, 0). \tag{7}$$

Step 5: Determination of vehicle status identifier $S_n(t)$ in next time step:

$$S_n(t + 1) = \begin{cases} 0 & \text{if } v_n(t + 1) > v_n(t) \\ S_n(t) & \text{if } v_n(t + 1) = v_n(t) \\ 1 & \text{if } v_n(t + 1) < v_n(t). \end{cases} \tag{8}$$

Step 6: Determination of time (t_{st}) stuck inside the jam:

$$t_{st} = \begin{cases} t_{st} = t_{st} + 1 & \text{if } v_n(t + 1) = 0 \\ t_{st} = 0 & \text{if } v_n(t + 1) > 0. \end{cases} \tag{9}$$

Step 7: Update position:

$$x_n(t + 1) = x_n(t) + \text{roundoff} \left(\frac{v_n(t) + v_n(t + 1)}{2} \right). \tag{10}$$

2.4. Lateral movement rules for cars

In real world, most road systems comprise at least two lanes and thus allow vehicles to change lane or make lateral displacement to overtake a slow vehicle in front. The first attempt for defining lane-change rules can be traced back to Rickert et al. [36]. According to their proposal, drivers will change lane only when the following two criteria are satisfied: (1) incentive criterion: the gap in front of one vehicle at the current lane should be no greater than its current speed and the gap in front of the adjacent lane should be larger than the current front gap; (2) safety criterion: any lateral displacement should not collide or block other vehicles behind. Therefore, the nearest neighbour lane must be empty and the maximum possible speed of the nearest vehicle behind on the other lane must be smaller than the gap between. In the following years, various lane-change rules were proposed. Recently, some interesting implementation thereof is also provided, for example, Jetto et al. [37] evaluated the traffic characteristics in front of multi-tollbooths with the prescribed lane-change rule. Nagel et al. [3], after surveying different lane-change rules, concluded that in spite of the difference among them, basically similar and realistic results were generated. This conclusion, however, may be valid only for pure traffic scenarios wherein all vehicles have identical size. In mixed traffic comprising cars and motorcycles, the lane-change behaviour will be different due to the complex interaction triggered by various maximum vehicular speeds as well as by different vehicular sizes (length and width).

Due to the fine cell system introduced, this study tries to divide the lateral movements for cars into two types: lane-change and lateral drift. The former refers to as a car (with 2 CUs in width) changing from one lane (with 3 CUs in width) to the neighbour lane (also with 3 CUs in width), for instance, from position 2 to 3 or from position 3 to 5 (see Fig. 2), whereas the later refers to as a car moving forward in the same lane but drifting from rightmost two sub-lanes to leftmost two sub-lanes (e.g., 4 → 6 or 5 → 7 in Fig. 2) or from leftmost two sub-lanes to rightmost two sub-lanes (e.g., 1 → 2 or 3 → 4 in Fig. 2). Both lane-change and lateral drift rules for cars are explained as follows.

Basically, the lane-change update rules for cars in mixed traffic follow that proposed by Hsu's et al. [33]. However, it is assumed that a lane change is only allowed when cars locate along the lane markings, such as positions 2, 3, 5, and 6 in Fig. 2. For cars located away from the lane markings, such as positions 1, 4, and 7 therein, it would take a little longer time to complete a lane change.

According to the proposed fine cell system shown in Fig. 2, a car (2 CUs in width) can locate either on the leftmost or rightmost 2 CUs (sub-lanes) within the lane (3 CUs in width) before making a lane change. For example, cars locating on the leftmost side of the left lane (e.g., position 1) would take slightly longer time to make a lane change than those on the rightmost side of the same lane (e.g., position 2). A car may require even longer time to make a lane change provided that the adjacent sites are occupied by motorcycles (e.g., position 4). There are two possibilities for a car to make a lane change:

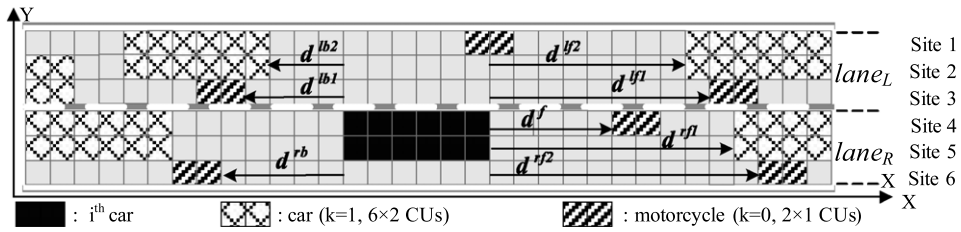


Fig. 3. Gaps evaluated by a car to perform either lane-change or lateral drift.

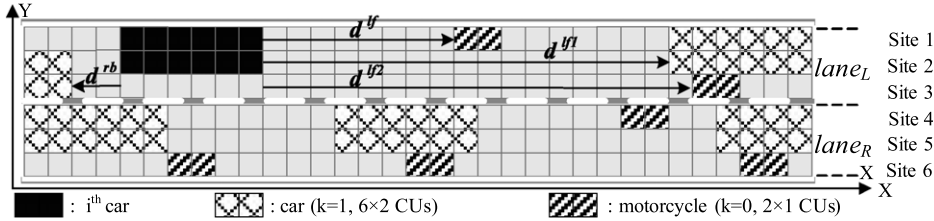


Fig. 4. Gaps evaluated by a car to perform lateral drift only.

the movements of $2 \rightarrow 3$ and $3 \rightarrow 5$ therein. After the lane change, it is assumed that in next time step the car will remain aligned with, but on the opposite side to, the lane markings. In a two-lane roadway, for example, if a car on the left lane wishes to change to the right lane, provided that no vehicles locate aside on the right lane, the lane-change CA rule can be expressed as

$$\begin{aligned}
 LC^{l \rightarrow r} : & \text{ If } v_{n+1}^r(t) > v_{n+1}(t) \text{ and } v_n(t) > v_{n+1}(t) \text{ and} \\
 & d_{n+1}^{eff,r}(t) > \min(d_n^{eff}, v_n(t+1)) \text{ and} \\
 & g_n^{r,b}(t) > v_n^{r,b}(t+1).
 \end{aligned} \tag{11}$$

In addition to the above lane-change behaviour, this study introduces another lateral movement “lateral drift” to further replicate the movement behaviour for cars in a fine cell system. The lateral drift behaviour happens when a car locating away from the lane markings intends to make a lane change (e.g., $1 \rightarrow 2 \rightarrow 3$ in Fig. 2) or when the car remains moving in the same lane but trying to overtake a slower motorcycle in front (e.g., $3 \rightarrow 4 \rightarrow 6$). In this study, when lateral drifts take place, cars remain within the same lane in next time step, as the movements of $1 \rightarrow 2$, $3 \rightarrow 4$, $4 \rightarrow 6$ and $5 \rightarrow 7$ in Fig. 2.

Upon above, we define the car’s lateral movements (lane-change or lateral drift) update rules as follows.

Step 1: incentive criteria. When cars move with positive speed and enjoy sizeable time headway to the front vehicle (say, 10 s), they will move forward with no lateral drift, since there is no incentive to do so. However, if there are vehicle(s) in near front, then different lateral movements may be triggered, depending on the sites they situate at present time. It is explained in Step 2.

Step 2: safety criteria. Check if situations around allow for lateral movements. Likely options for cars’ lateral movements will depend on the original position.

Step 2A: when cars move aside the lane markings (e.g., the car marked in black in Fig. 3), both lane-change and lateral drift are likely to take place depending on the traffic situation around. The following sub-steps for lateral movements are applied (see Fig. 3):

Step 2A-1: check the gaps backward on both sides (d^{lb1} , d^{lb2} and d^{rb}) to determine if a lateral movement is allowed. The rationale for considering both d^{lb1} and d^{lb2} is that in mixed traffic context the next two sites behind (for instance, site 2 and site 3 in Fig. 3) in the target lane may be occupied by different vehicles with different speeds. Hence, both sites must be evaluated to find out the exact backward gap.

Step 2A-2: when with allowable gaps backward, check the front gaps if a lane-change or a lateral drift is taken so as not to be hindered by a slow vehicle in front. For example, for the designated car in Fig. 3, five gaps (d^{lf1} , d^{lf2} , d^{lf} , d^{rf1} and d^{rf2}) must be evaluated to determine the best option to be taken. In the case that both options are allowed, the one with longer gap, i.e., more advantageous, will be selected. Also be aware that the front gaps are the effective gaps in next time step, as defined by Knospé [6] to catch more precisely the real traffic condition.

Step 2B: when cars move along the side lane away from the lane markings (e.g., the car marked in black in Fig. 4), only the lateral drift is considered because lane change could be taken only after the car drifting to the right side of the lane it locates. Consequently, the following sub-steps apply for a car’s lateral drift (see Fig. 4):

Step 2B-1: check the space backward on the inner side (d^{rb}) to determine if a car lateral drift is allowed.

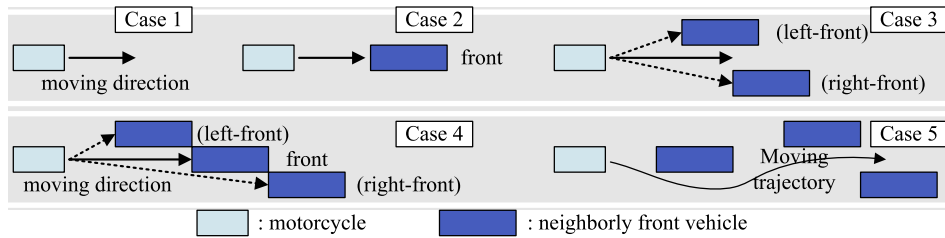


Fig. 5. Field observed motorcycle's possible movements.

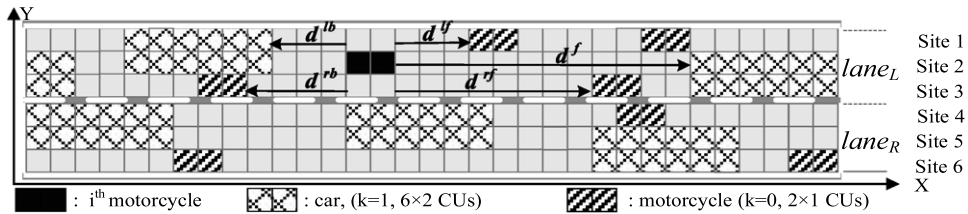


Fig. 6. Gaps evaluated by a motorcycle to perform lateral drift from the middle site.

Step 2B-2: when with allowable gap backward, check the minimum front gap if a lateral drift is to be taken for not being hindered by a slow motorcycle in front. For example, d^{lf1} , d^{lf2} and d^f require being evaluated.

2.5. Lateral movement rules for motorcycles

Unlike most cars which will move within the lane, motorcycles in practice do not follow the lane disciplines. From the field observation one can easily find that motorcycles in effect move in a rather erratic manner without obeying the lane disciplines. Sometimes the motorcycles follow the lead vehicles; but more than often, they share the “same lane” with the moving cars or break into two moving cars in the same lane. During traffic jams, some motorcycles, once blocked ahead, even cross the gap between two queued cars with a wide transverse displacement to keep moving (see Fig. 1). This evidence justifies the non-lane-based movements for motorcycles. Based upon field observation by Lan and Chang [32], possible motorcycle movements can be categorized into five classes, as shown in Fig. 5.

In a moving traffic condition, although different movements of motorcycles can be identified, the lateral displacement is basically characterized as a motorcycle's lateral drift—displace one site laterally in next time step. In this case, the lateral movement update rule for motorcycles is a simplified version of the counterpart for cars, which can be described as follows.

- Step 1: incentive criterion. It is identical to that for cars. When a motorcycle enjoys sizeable time headway to the front vehicle, no lateral displacement will be activated. Next, if there is a vehicle in near front on the same sub-lane, either drifting to the left sub-lane or the right sub-lane could be chosen, depending on the position it situates at present time. It is explained in Step 2.
- Step 2: safety criterion. Check if situation around allows a lateral drift. However, available options for a motorcycle's lateral drift will depend on the original position.
 - Step2A: when a motorcycle locates in the middle sub-lane (e.g., site 2, 3, 4, or 5 in Fig. 6), lateral drifts to both outer and inner sites are feasible. Therefore, the following sub-steps require further examination.
 - Step 2A-1: check the gaps backward on both sides. For instance, for the designated motorcycle marked in black in Fig. 6, backward gaps d^{lb} and d^{rb} require being evaluated to determine if a lateral drift is allowed.
 - Step 2A-2: when with allowable gaps in the back, check the front gaps if a motorcycle's lateral drift is to be taken. For example, for the designated motorcycle in Fig. 6, three gaps (d^{lf} , d^{rf} and d^f) are evaluated to determine the best drift option. Similar to cars, in the case that both options are allowed, the lateral drift option with larger gap is chosen.
 - Step 2B: when a motorcycle locates on the innermost or outermost sub-lane (i.e., site 1 or 6 in Fig. 7), only drifting inboard is available. Taking the motorcycle marked in black in Fig. 7 as an example, the only lateral drift option is from site 1 to site 2. The following two sub-steps apply:
 - Step 2B-1: check the gaps backward on left side (d^{rb}) to determine if a motorcycle's lateral drift is allowed.
 - Step 2B-2: when with an allowable gap in back, check the minimum front gap should a motorcycle's lateral drift be taken. d^{lf} , and d^f must be evaluated.

Another unique feature for motorcycles is the “transverse crossing”, which is frequently observed when motorcycles are stuck in traffic or forced to halt in front of signalized intersections. The possible options for transverse crossing behaviour are demonstrated in Fig. 8 with update CA rules described as follows.

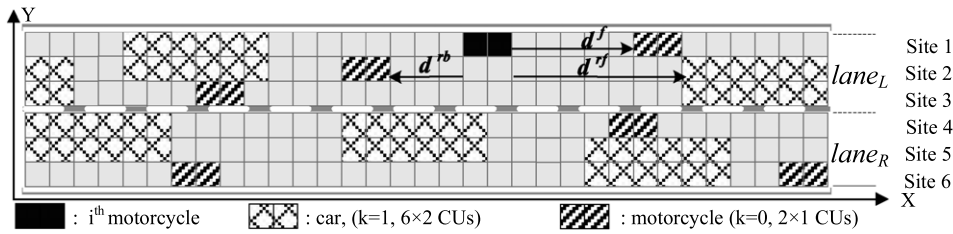


Fig. 7. Gaps evaluated by a motorcycle to perform lateral drift from the outermost site.

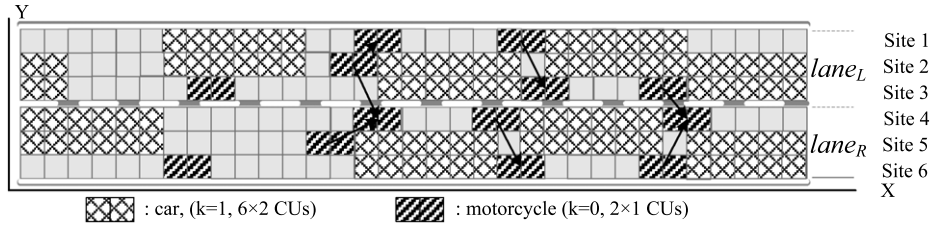


Fig. 8. Transverse crossing behaviour for motorcycles when stuck in traffic.

- Step 1: incentive criterion. When a motorcycle is stuck in traffic jam and remains stationary for a certain period (say, 3 s), there is an incentive for the motorcycle to take a transverse crossing through the gap between two queued vehicles, either to the left or to the right sub-lane, in order to keep moving as forward as possible.
- Step 2: safety criterion. Check if situations around allow for a transverse crossing. First, check if the next left or right sub-lane in front is occupied. If no, then evaluate the forward and backward condition on the target sub-lane whether a transverse crossing is allowed. In the case the next sub-lane in front is also occupied then check the next second sub-lane whether the backward and forward condition allows for taking a transverse crossing. When both left and right sub-lanes allow for a transverse crossing maneuver, select the option that is most advantageous.

3. Simulations

3.1. The simulated scenarios

The simulations are performed on a closed track containing 6×1800 site CUs, which represents a two-lane roadway section of width 7.5 m and length 1800 m. Both pure traffic and mixed traffic scenarios are simulated. The pure traffic scenario (cars only) simulates the freeway context; whereas the mixed traffic scenario (cars and motorcycles) simulates the urban surface road context. We simulate for 600 time steps. Initially, all the vehicles are set equally spaced or lined up from the end of the road section on the circular track, with speed 0 at time step 0. For pure traffic simulation in the freeway, the maximum speed for cars is set according to the speed limits (110 kph) prevailing in Taiwan, that is, 31 cells/s. For mixed traffic simulation in the surface road, the maximum speed is set as 17 cells/s (60 kph) for cars and 14 cells/s (50 kph) for motorcycles, respectively.

3.2. Pure car traffic

In order to analyze the effects of car lateral drift behaviours on traffic flow, we simulate the scenarios identical to Lan et al. [34], namely, pure car traffic on a periodic boundary 2-lane freeway roadway of length 1800 m with maximum speed of 31 cell/s. All the parameter settings remain unchanged except that in this sophisticated CA model the probability of cars' lateral drifts (P_{ld}) is set as 0.5. When simulations begin ($t = 0$), cars are equally spaced but randomly locate on outer or inner side of both lanes. The derived simulation results are then compared with those without introducing cars' lateral drift. Fig. 9 presents the derived flow-occupancy relations (fundamental diagrams).

As shown in Fig. 9, both fundamental diagrams, with and without car drifts, are similar. Introducing the car lateral drift behaviour will slightly lower the maximum flow, however. This is due to the rule that cars locating away from the lane markings need to take a little longer time (2 time steps) to make a lane change. However, there is less incentive for cars to take a lateral drift within the lane because there are no side motorcycles sharing (disturbing) the same lane. Our results concur with Nagel et al. [3] in spite of different lane-change rules being introduced.

3.3. Mixed traffic scenario

For mixed traffic scenario with prevalence of cars and motorcycles, the effects of car's lateral drifts should be more significant due to the complicated interactions between cars and motorcycles triggered. We examine the mixed traffic CA

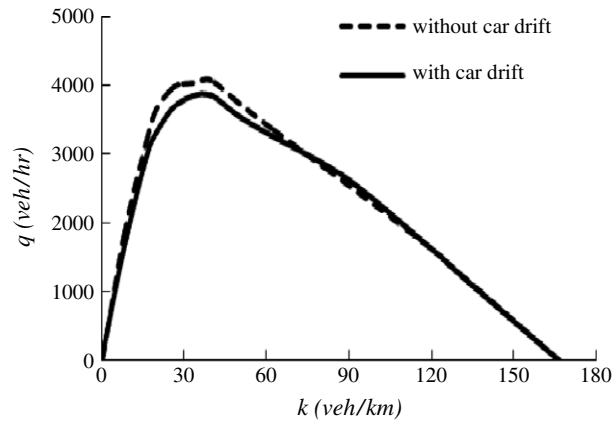


Fig. 9. Fundamental diagrams for cars in pure traffic with and without lateral drifts.

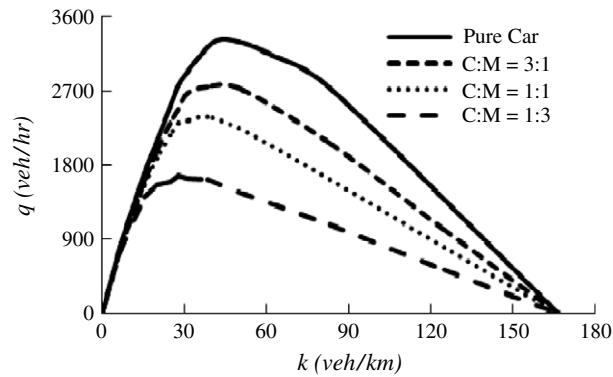


Fig. 10. Fundamental diagrams for cars in mixed traffic under various $C:M$ ratios.

simulations under different car-motorcycle ratios (hereinafter, $C:M$). Owing to the complex nature of mixed traffic, one should be aware that even for a given occupancy $\rho(S)$, the mixed traffic may be composed of different $C:M$ ratios. Given that one car always occupies 6×2 CUs, six times as large as one motorcycle which occupies 2×1 CUs, and that our simulations are performed on a closed track containing 6×1800 CUs, for a given occupancy, the relationship between number of cars (NC) and number of motorcycles (NM) can be expressed as a linear relationship as Eq. (12):

$$6NC + NM = 5400 * \rho(S). \quad (12)$$

In order to analyze the impacts of motorcycles' lateral drift and transverse crossing behaviour on the traffic, we deliberately fix the number of cars in each simulation and choose three $C:M$ ratios (1:3, 1:1 and 3:1) for the following experiments. When initiating the simulations, cars line up from the end of the road section in the left two sub-lanes of both lanes, while motorcycles line up aside in the right sub-lane of both lanes. Fig. 10 is the derived fundamental diagrams wherein the vertical axis represents the car traffic flow and the horizontal axis shows the car occupancy (density). One may find that as the number of motorcycles increases, larger deterioration of car flow has been identified. This phenomenon indicates that introduction of more slow motorcycles will inevitably impair the cars' movement and thus results in a lower traffic flow.

This phenomenon can be further illustrated through the simulated $x-t$ plots, as shown in Fig. 11, with fixed car density ($\rho_c = 50$ veh/ln/km) in various $C:M$ ratios. Both the trajectories of cars and motorcycles are displayed in Fig. 11 where X -axis represents the time, advancing from left to right, and Y -axis represents positions of vehicles, moving from bottom to top. For ease of distinguishing, the head positions of motorcycles are shown in blue dots and cars in black dots therein. As shown in Fig. 11(b)–(d), it is clear that even for low $C:M$ ratios, the car platoons preset at $t = 0$ will disperse quickly as time marches. This phenomenon significantly differs from that in the $x-t$ plot for pure car traffic, as shown in Fig. 11(a). It is clear that when motorcycles in front with lower average speed will seriously impair the cars embarking from the downstream front of the initial platoon and, henceforth, on average, cars have to take longer time to arrive at the upstream front of the initial platoon. Consequently, the car platoon shrinks quickly and disperses in shorter time, implying a lower traffic flow for cars.

We further simulate similar scenarios proposed by Meng et al. [19]. For comparison, we select identical motorcycle densities to those set by Meng et al. [19]. According to Fig. 12(a), it is found that the derived car flow profiles are similar.

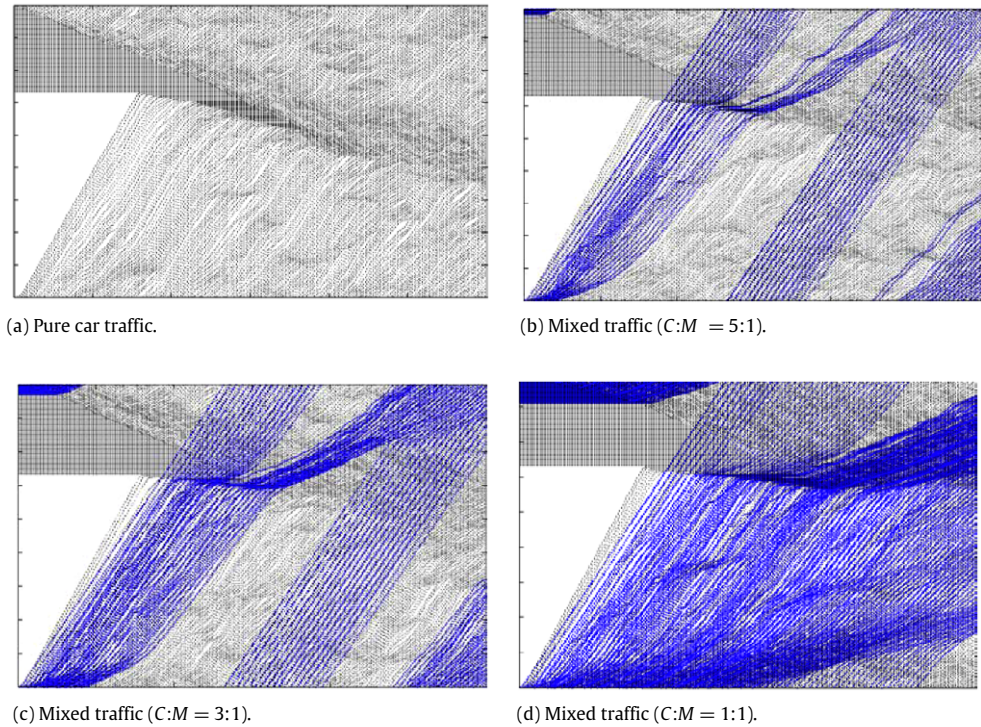


Fig. 11. $x-t$ plots in mixed traffic with different $C:M$ ratios (car density $\rho_c = 50$ veh/ln/km).

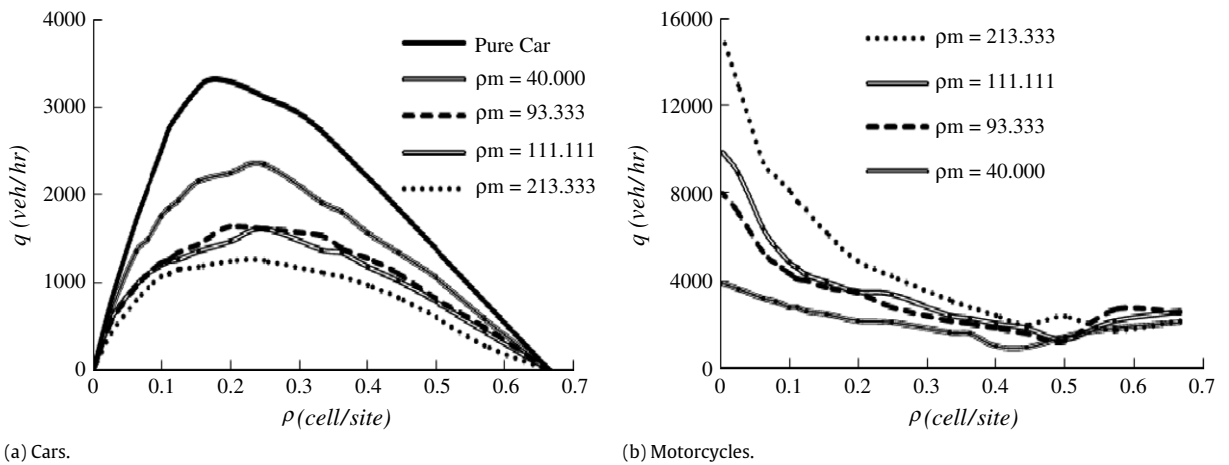


Fig. 12. Fundamental diagrams for cars and motorcycles under various motorcycle densities.

Car flow constantly decreases as more motorcycles are introduced because of more interference to cars. In contrast, on each motorcycle curve (with fixed motorcycle density) shown in Fig. 12(b), motorcycle flow also decreases as more cars are introduced. This phenomenon is consistent with the general rule that more congested traffic would couple with a lower flow.

Furthermore, our simulation reveals that for pure motorcycle traffic, motorcycle flow increases as motorcycle density rises. The reason for this is that since there are six sites available in lateral in the simulated roadway, the motorcycle traffic pattern remains free flow even if motorcycle density (ρ_m) has reached 213 veh/ln/km (or 35.5 veh/site/km). Our simulation also shows that with high car densities, motorcycle flow will converge to a certain margin, regardless of the preset motorcycle density. This could be induced as the coupled effect of car's lateral drifts and motorcycle's lateral drifts as well as transverse crossings, interpreted as follows.

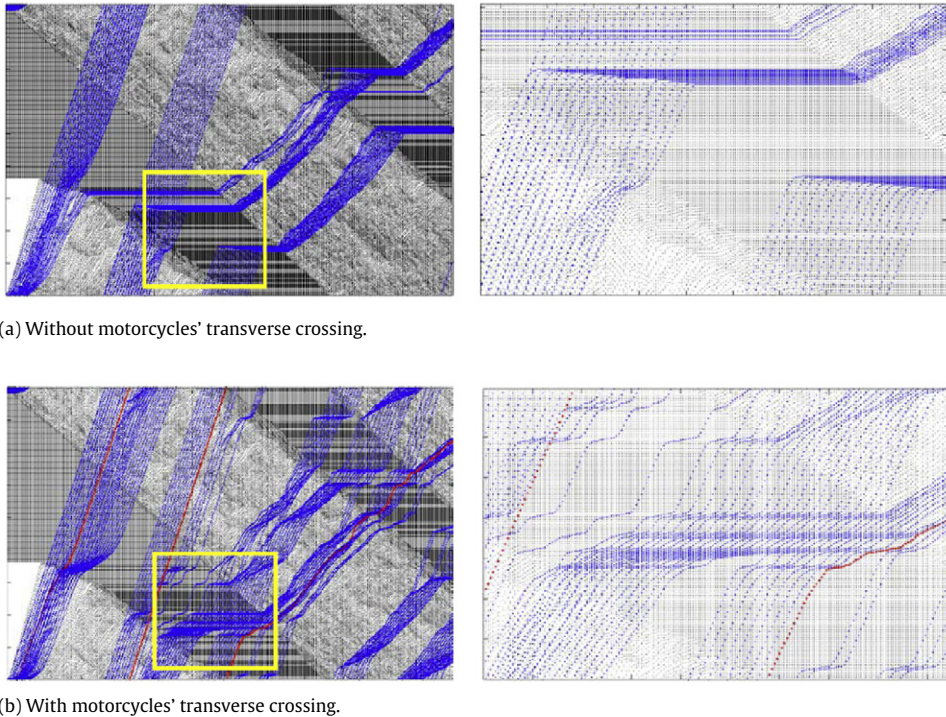


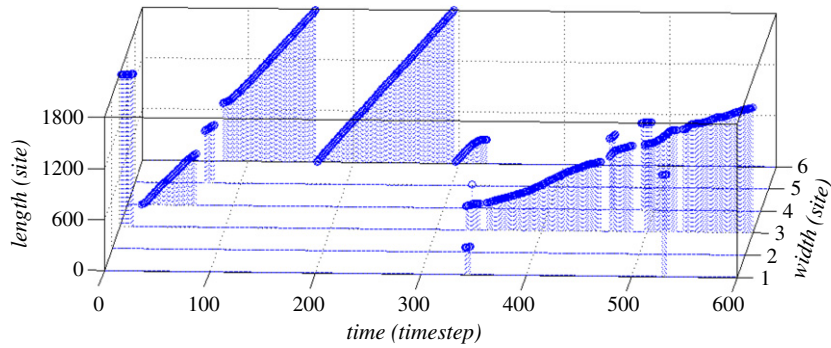
Fig. 13. $x-t$ plots in mixed traffic with and without motorcycles' transverse crossing ($\rho c = 100$ veh/ln/km, $\rho m = 10$ veh/ln/km). The right panels zoom out the vehicular trajectories in the area marked in the left panels. The designated motorcycle is marked in red. (For interpretation of the references to colour in this figure legend, the reader is referred to the web version of this article.)

In high car densities where the road section is almost occupied by cars (e.g., $\rho > 0.6$, or $\rho c > 150$ veh/ln/km), owing to the car's lateral drift behaviour, cars locate randomly on either left or right two sub-lanes of each lane, which stand as obstacles to the motorcycles. Nevertheless, owing to the unique features of motorcycle's lateral drift and transverse crossing behaviours, motorcycles can always move further if situations allow. However, since a slow car in right front will serve as a fixed or moving bottleneck for motorcycles, a converged trend for motorcycle flow is eventually observed. This also coincides with the previous works [34,38] that when bottleneck is introduced, a plateau regime may be identified in the mid-density range.

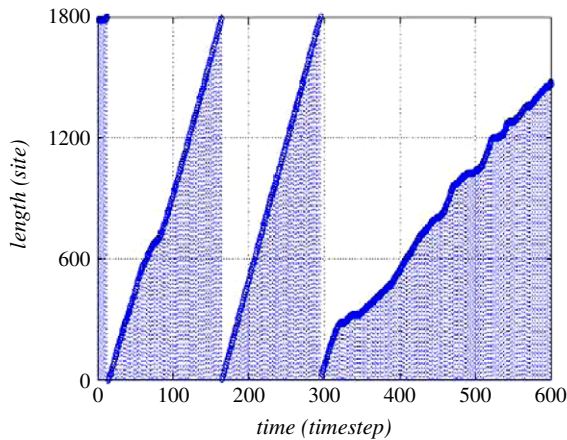
The lateral drift and transverse crossing behaviours of motorcycles can be further demonstrated through the simulated $x-t$ plots, as shown in Fig. 13. The scenario simulated is under $\rho c = 100$ veh/ln/km (congested traffic). As the simulation starts, cars line up from the end of the road section on the left side of both lanes so as to form the initial car platoons. To clearly demonstrate the motorcycle trajectories in such congested traffic conditions, only few motorcycles (say, 10 veh/ln/km) are introduced, which also line up next to the car platoons on the right empty sub-lane of each lane.

In Fig. 13 both trajectories of cars and motorcycles are displayed, either with or without consideration of motorcycle's transverse crossing behaviour. In Fig. 13(a), one can find that motorcycles break into the traffic jam when arriving at the upstream front as long as there is one empty site available laterally in each lane. However, due to the car's lateral drift effect, when there is a car blocking the front site, motorcycles will get stuck in traffic jam until the front stationary cars reach the downstream front of traffic jam. In contrast, if the motorcycle's transverse crossing behaviour is introduced, as shown in Fig. 13(b), one can find the similar situation that motorcycles break into the traffic jam from its downstream front. But they are also capable of making transverse crossings to the next or next second sub-lane, even blocked by a stationary car in front, provided that the situations allow. After that, motorcycles continuously move forward in consecutive time steps until confronting another stationary car in front that may force them to take another transverse crossing again.

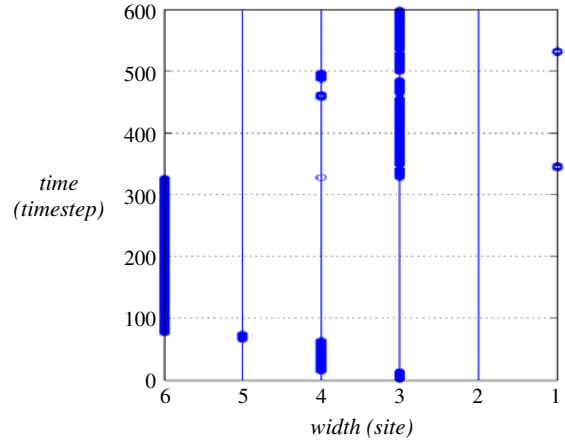
Fig. 14 further demonstrates the trajectory, both the longitudinal and lateral position, of a designated motorcycle marked in red in Fig. 13(b). According to Fig. 14, one may find that when simulation initiates, cars line up on the left two sub-lanes from the end of the circular track and leave the right sub-lane empty; therefore, in the early time steps, motorcycles can easily break into the initial car platoon from its upstream front and smoothly move forward. As a consequence, only few motorcycle's transverse crossings can be observed. As time marches, more frequent car lateral drifts are triggered and henceforth transform into more bottlenecks for motorcycles. This means that there are increasing occasions that motorcycles have to take transverse crossings through the stationary cars to move as forward as possible in later time steps. This phenomenon can be supported by the significant difference of number of transverse crossings for the designated motorcycle in the first simulated 150 s and in the latter time steps ($t = 300-600$ s). To recap, the simulated results have precisely



(a) 3-dimensional motorcycle's trajectory.



(b) Longitudinal position vs. time.



(c) Lateral position vs. time.

Fig. 14. The trajectories of the designated motorcycle marked in red in Fig. 13(b).

reflected the real traffic features in mixed traffic contexts. The results also reveal the importance of introducing motorcycle's transverse crossing behaviour into the simulations, especially in congested mixed traffic.

4. Conclusion

This study extends our earlier work [34] by further developing a sophisticated CA model to simulate the mixed traffic comprising cars and motorcycles. Owing to the enhanced resolution of finer cell system, slight speed variations and effects of both the vehicular length and width can be simulated. Most importantly, the frequently observed lateral movements of cars and motorcycles as well as the wide transverse crossing behaviour of motorcycles are carefully deliberated with the corresponding CA update rules thereby added. Comparisons with existing studies authenticate the validity of our sophisticated CA model while simulating the pure car traffic scenarios. The simulations show that the unique lateral movements of motorcycles that yet investigated in any existing studies, such as breaking into two moving cars and transverse crossing through two stationary cars in traffic jam, can be precisely illustrated. Our simulations reveal the prevailing motorcycle's transverse crossing behaviour in mixed congested traffic. The maximum car flow decreases with the increase of motorcycle density because the increased interaction among different vehicles will impair the flow efficiency. This conclusion agrees with the study of Meng et al. [19].

Several avenues can be identified for future study. In this study the car locating away from the lane markings is assumed taking two time steps to make a lane change. This is deemed a conservative restriction. Moreover, each vehicle only evaluates the traffic conditions around for the next one or two time steps could also be too conservative. One possible remedy is introducing the anticipation of surrounding conditions with more extended time steps. Next, according to our field observations, there is significant heterogeneity in the maximum speeds among different motorcyclists, which leads to frequent lateral drift behaviours in non-congested flow. Therefore, the effect of various maximum speeds for motorcycles can be considered in the further study. Finally, in real world a car is possible to locate in the center area of each lane, a little different from either left or right two sub-lanes as described in this study. This may further discourage the aside motorcycles from sharing the same lane. To deal with this phenomenon, implementation of the more refined cell system might be necessary. It, however, will significantly increase the computation burden and require more simulation time. A trade-off between simulation efficiency and realism of simulation deserves further evaluation.

Table A.1
Notation table.

Variable/parameter	Definition
S	Spatiotemporal domain under consideration with size $L \times W \times T$
L	Longitudinal length of S
W	Transverse width of roadway
T	Observed time period
$q(S)$	Generalized traffic flow over S
$\rho(S)$	Generalized occupancy over S
$ S $	'Volume' of S
$N_0(t)$	Total number of sites occupied by cells (vehicles) at the instantaneous time t
N	Total number of sites arranged in domain S
t	Time:
$t(S)$	Accumulated of $N_0(t)$ for all times simulated
$t_h = d_n/v_n(t)$	Time headway of n th vehicle to front
h_k	Preset time threshold of vehicle of type k for reflecting effect of synchronized distance
$t_s = \min(v_n(t), h_k)$	Final time threshold for initiating the consideration of front brake light effect, as take vehicular speed into consideration
t_{st}	Accumulated time of vehicle stuck in traffic jam
$t_{k,c}$	Time threshold of vehicle of type k for initiating the delay-to-start behavior
τ	Safe time gap for collision prevention
P	Probability:
P_b	Accounting for impact of decelerating vehicle in near front
P_0	Reflect the delay-to-start behaviours of vehicles stuck in traffic jam
P_d	Other situations
P_{lc}	Probability of lane-change
P_{ld}	Probability of lateral drift
d	Space headway
$d(S)$	The total distance travelled by all cells in S
d_n^{eff}	Effective distance of n th vehicle
g	Distance (Gap)
x	Position of n th vehicle
v	Speed
$v(S)$	Generalized space-mean speed over S
c_n	Safe speed of n th vehicle
a_k	Maximum acceleration capacity of k -type vehicle
D	Maximum deceleration capacity of k -type vehicle
rand()	Randomly generated number
S_n	Status identifier of n th vehicle, representing its brake light status
Δ	Minimum clearance for the follower
NC	Number of cars in the mixed traffic of given $\rho(S)$
NM	Number of motorcycles in the mixed traffic of given $\rho(S)$
Suffix	
n	n th vehicle
$n + 1$	Vehicle in front
k	Type of vehicles: $k = 0$, motorcycle; $k = 1$, car
max	The maximum value
Superscript	
$r(l)$	The right (left) lane or site considered for a lane change or a lateral drift
f	Downstream
b	The nearby upstream in the next or next second site
$1(2)$	The next (the next second) site considered for a lateral movement

Acknowledgements

The authors wish to thank two anonymous referees for their insightful comments and constructive suggestions. This research was granted by National Science Council, Republic of China (NSC 95-2211-E-451-015-MY3).

Appendix

See Table A.1.

References

- [1] K. Nagel, M. Schreckenberg, J. Phys. I France 2 (1992) 2221.
- [2] K. Nagel, Phys. Rev. E 53 (5) (1996) 4655.
- [3] K. Nagel, D.E. Wolf, P. Wagner, P. Simon, Phys. Rev. E 58 (2) (1998) 1425.
- [4] D. Chowdhury, D.E. Wolf, M. Schreckenberg, Physica A 235 (1997) 417.
- [5] R. Barlović, L. Santen, A. Schadschneider, M. Schreckenberg, Eur. Phys. J. B 5 (1998) 793.
- [6] W. Knosp, L. Santen, A. Schadschneider, M. Schreckenberg, J. Phys. A 33 (2000) L477.

- [7] R. Jiang, Q.S. Wu, J. Phys. A 36 (2003) 381.
- [8] G.H. Bham, R.F. Benekohal, Transp. Res. C 12 (2004) 1.
- [9] M.E. Lárraga, J.A. Del Río, L. Alvarez-Icaza, Transp. Res. C 13 (2005) 63.
- [10] D. Chowdhury, L. Santen, A. Schadschneider, Phys. Rep. 329 (2000) 199.
- [11] B.S. Kerner, H. Rehborn, Phys. Rev. E 53 (5) (1996) R4275.
- [12] B.S. Kerner, S.L. Klenov, J. Phys. A 35 (2002) L31.
- [13] B.S. Kerner, S.L. Klenov, D.E. Wolf, J. Phys. A 35 (2002) 9971.
- [14] B.S. Kerner, The Physics of Traffic, Springer, Berlin, New York, Tokyo, 2004.
- [15] A. Ebersbach, J. Schneider, I. Morgenstern, R. Hammwohner, Internat. J. Modern Phys. C 11 (4) (2000) 837.
- [16] R. Wang, R. Jiang, Q.S. Wu, M. Liu, Physica A 378 (2007) 475.
- [17] H. Ez-Zahraouy, K. Jetto, A. Benyoussef, Eur. Phys. J. B 40 (2004) 111.
- [18] B.S. Kerner, S.L. Klenov, J. Phys. A 37 (2004) 8753.
- [19] J.P. Meng, H.Q. Dai, L.Y. Dong, J.F. Zhang, Physica A 380 (2007) 470.
- [20] O. Biham, A.A. Middleton, D.A. Levine, Phys. Rev. A 46 (10) (1992) R6124.
- [21] J. Esser, M. Schreckenberg, Internat. J. Modern Phys. C 8 (5) (1997) 1025.
- [22] P. Simon, K. Nagel, Phys. Rev. E 58 (2) (1998) 1286.
- [23] D. Chowdhury, A. Schadschneider, Phys. Rev. E 59 (2) (1999) R1311.
- [24] M.S. Watanabe, Physica A 324 (2003) 707.
- [25] M.S. Watanabe, Physica A 328 (2003) 251.
- [26] X.Q. Shi, Y.Q. Wu, H. Li, R. Zhong, Physica A 385 (2007) 659.
- [27] S. Feng, G. Gu, S. Dai, Commun. Nonlinear Sci. Numer. Simul. 2 (2) (1997) 70.
- [28] B. Chopard, A. Dupuis, P.O. Luthi, Workshop. Traffic and Granular Flow, World Scientific Publishers, 1997, 153.
- [29] R. Jiang, Q.S. Wu, Physica A 364 (2006) 493.
- [30] G.L. Xiong, Y. Huang, Syst. Eng. 24 (6) (2006) 24 (in Chinese).
- [31] I. Spyropoulou, Transp. Res. C 15 (2007) 175.
- [32] L.W. Lan, C.W. Chang, J. Adv. Transp. 39 (2005) 323.
- [33] C.C. Hsu, Z.S. Lin, Y.C. Chiou, L.W. Lan, J. Eastern Asia Soc. Transportation Stud. 7 (2007) 2246.
- [34] L.W. Lan, Y.C. Chiou, Z.S. Lin, C.C. Hsu, Physica A 388 (2009) 3917–3930.
- [35] H.K. Lee, R. Barlovic, M. Schreckenberg, D. Kim, Phys. Rev. Lett. 92 (2004) 238702.
- [36] M. Rickert, K. Nagel, M. Schreckenberg, A. Latour, Physica A 231 (1996) 534.
- [37] K. Jetto, H. Ez-Zahraouy, A. Benyoussef, Internat. J. Modern Phys. C. 19 (2008) 903.
- [38] H.B. Zhu, L. Lei, S.Q. Dai, J. Phys. A 388 (2009) 2903.